Discussion of Cold Nuclear Matter Effects on Quarkonium Production

R. Vogt

Physics Division, Lawrence Livermore National Laboratory, Livermore, CA 94551, USA

Physics Department, University of California, Davis, CA 95616, USA

(Cold) Nuclear Matter Influences Final-State Quarkonium Production

Cold matter effects are non-QGP effects: form baseline features of nuclear collisions

Hard processes, like quarkonium production, should have a linear A dependence if no nuclear effects, $\sigma_{pA} = \sigma_{pp} A$

Instead

$$\sigma_{pA} \propto \sigma_{pp} A^{\alpha}$$

where the exponent α characterizes the difference between the measured behavior in the nucleus and that expected from hard interactions — 'kitchen sink' approach

- **Fixed-target experiments show that A dependence of J/ψ production is less than linear ($\alpha < 1$)**
- **J/ψ and ψ' A dependencies are different**
- **Inclusive J/ψ has contributions from χ_c and ψ' feed down**
- **Initial-state parton distributions in nuclei are different than in free protons**

A Dependence of J/ψ and ψ' Not Identical

High statistics data sets (NA50 at SPS, E866 at FNAL) show clear difference at midrapidity [NA50 ρL fit gives $\Delta\sigma = \sigma^{\psi'}_{\rm abs} - \sigma^{J/\psi}_{\rm abs} = 4.2 \pm 1.0$ mb at 400 GeV, 2.8 ± 0.5 mb at 450 GeV for absolute cross sections], size matters!

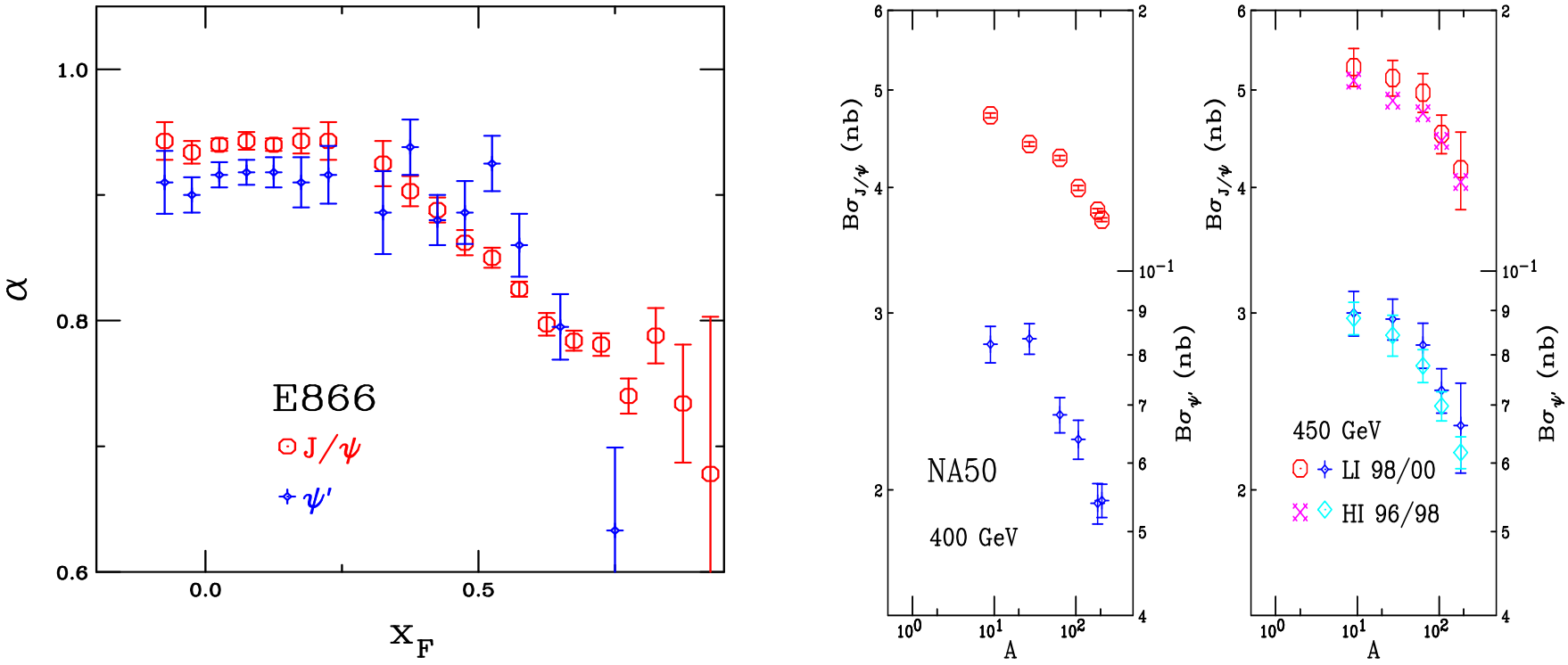

Figure 1: **The J/ψ A dependence (left) as a function of x_F at FNAL ($\sqrt{s_{NN}} = 38.8$ GeV) and (right) and a function of A at the SPS (NA50 at $p_{\rm lab} = 400$ and 450 GeV) for J/ψ and ψ' production.**

Parton Densities Modified in Nuclei

Nuclear deep-inelastic scattering measures quark modifications directly, gluon modifications only through Q^2 dependence of F_2

More uncertainty in nuclear gluon distribution, relies also on momentum conservation

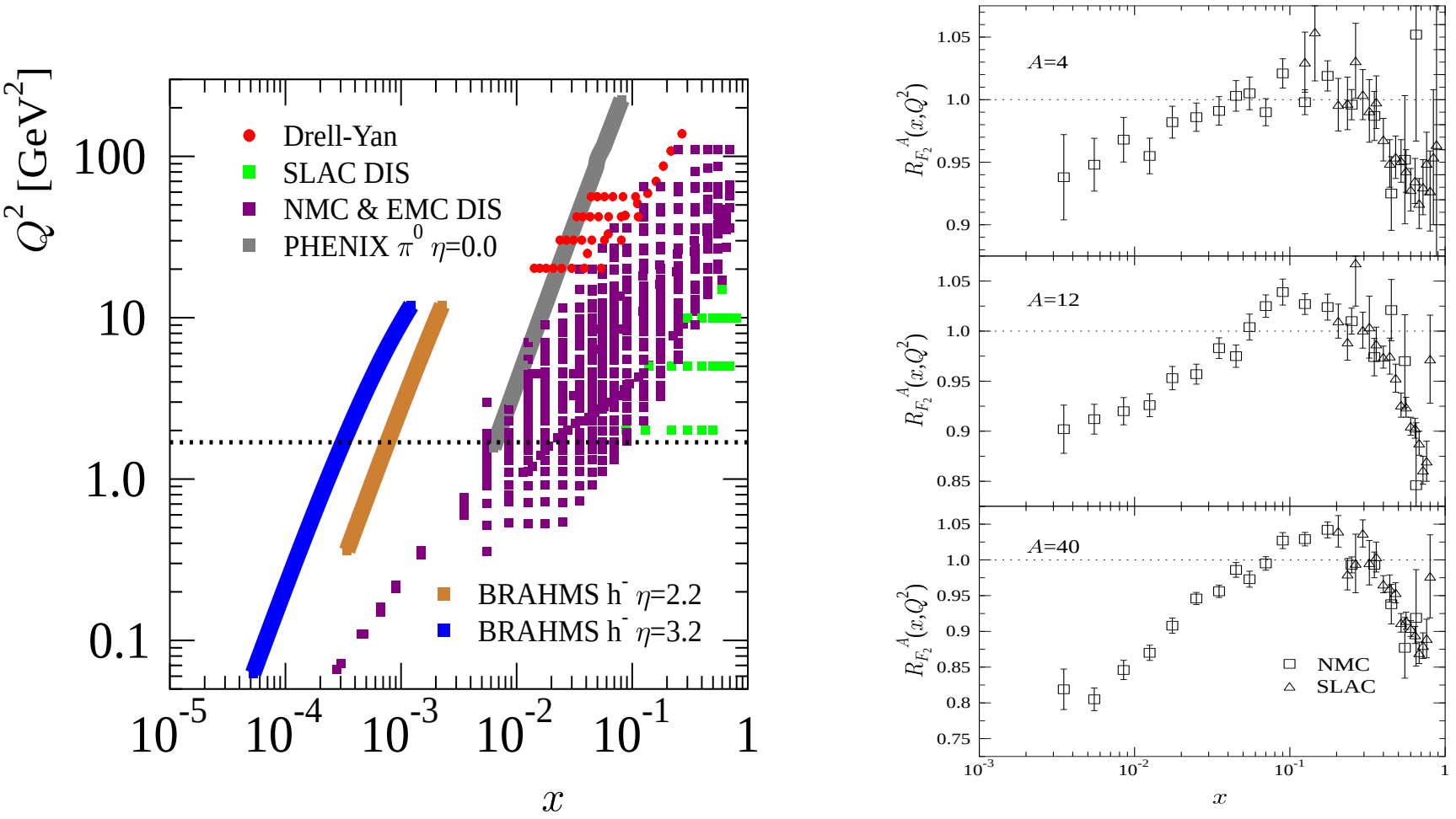

Figure 2: Left: x and Q^2 range of EPS09 analysis. Right: Ratios of charged parton densities in He, C, and Ca to D as a function of x. [From K.J. Eskola.]

What Are Cold Matter Effects?

Important cold nuclear matter effects include initial and final state effects:

- **Initial-state nuclear effects on the parton densities (shadowing)**
- **Initial-state energy loss**
- **Intrinsic heavy flavors (see paper by Brodsky and Lansberg on IC in RHIC pp collisions)**
- **Final-state absorption on nucleons**

Shadowing and absorption most important at midrapidity, initial-state energy loss and intrinsic heavy flavor more important at forward rapidity

Production mechanism affects both intimately:

- **Shadowing depends on momentum fraction x of the target (and projectile in AA) which is influenced by how the state was produced: $2 \to 1$ or $2 \to 2$ process [CEM vs. CSM (Ferreiro *et al.*)]**
- **Production affects absorption because singlet and octet states can be absorbed differently**

Quantifying Cold Matter Effects

Fixed-target experiments usually report heavy-to-light ratios or extract exponent α and plot as a function of A for integrated results or x_F/y for more differential; as a function of $N_{\rm coll}$ or $N_{\rm part}$ (or nuclear path length L at CERN SPS) for centrality studies

Heavy-Light Ratios, $R_{BA}(x_F/y)$: x_F/y-dependent per-nucleon ratios

$$\frac{\sigma_{pA}(\sqrt{s_{_{NN}}}, x_F/y)}{\sigma_{pp}(\sqrt{s_{_{NN}}}, x_F/y)} \propto \frac{1}{A}\frac{f_g^A(x,\mu^2)}{f_g^p(x,\mu^2)}$$

Probes ratio of gluon distributions at same x for a given x_F or y when pA and pp collisions at the same value of $\sqrt{s}$, different x values probed if $\sqrt{s} \neq \sqrt{s_{_{NN}}}$

Centrality-dependent Ratios:

- **In a given rapidity region show centrality dependence; in a pA collision, $T_{AB}, N_{\rm part} \to T_A$, the nuclear profile function**

$$R_{AB}(N_{\rm part}; b) = \frac{d\sigma_{AB}/dy}{T_{AB}(b) d\sigma_{pp}/dy}\ ; \qquad T_{AB}(b) = \int d^2s dz dz' \rho_A(s,z)\rho_B(|\vec{b}-\vec{s}|, z')\ ; \qquad T_A(b) = \int dz \rho_A(s,z)$$

$$N_{\rm part}(b) = \int d^2s \left[T_A(s)(1-\exp[-\sigma_{\rm inel}(s_{_{NN}})T_B(|\vec{b}-\vec{s}|)]) + T_B(|\vec{b}-\vec{s}|)(1-\exp[-\sigma_{\rm inel}(s_{_{NN}})T_A(s)])\right]$$

- **Central to peripheral ratio, compare two centrality regions vs. rapidity**

$$R_{CP}(y) = \frac{T_{AB}(b_P)}{T_{AB}(b_C)}\frac{d\sigma_{AB}(b_C)/dy}{d\sigma_{AB}(b_P)/dy}$$

Nuclear Parton Distributions

Nuclear parton densities

$$\begin{aligned} F_i^A(x,Q^2,\vec{r},z) &= \rho_A(s) S^i(A,x,Q^2,\vec{r},z) f_i^N(x,Q^2) \\ s &= \sqrt{r^2+z^2} \\ \rho_A(s) &= \rho_0 \frac{1+\omega(s/R_A)^2}{1+\exp[(s-R_A)/d]} \end{aligned}$$

With no nuclear modifications, $S^i(A,x,Q^2,\vec{r},z) \equiv 1$

When studying impact parameter, b**, dependent observables, assume spatial dependence proportional to nuclear path length:**

$$S_\rho^i(A,x,Q^2,\vec{r},z) = 1 + N_\rho(S^i(A,x,Q^2)-1)\frac{\int dz \rho_A(\vec{r},z)}{\int dz \rho_A(0,z)}$$

Normalization: $(1/A)\int d^2r dz \rho_A(s) S_\rho^i \equiv S^i$**. Larger than average modifications for** $s=0$**. Nucleons like free protons when** $s \gg R_A$**.**

Shadowing Parameterizations On The Market

EKS98: K. J. Eskola, V. J. Kolhinen and P. V. Ruuskanen, Nucl. Phys. B 535 (1998) 351 [arXiv:hep-ph/9802350]; K. J. Eskola, V. J. Kolhinen and C. A. Salgado, Eur. Phys. J. C 9 (1999) 61 [arXiv:hep-ph/9807297].

nDS: D. de Florian and R. Sassot, Phys. Rev. D 69, 074028 (2004) [arXiv:hep-ph/0311227].

HKN: M. Hirai, S. Kumano and T. H. Nagai, Phys. Rev. C 70, 044905 (2004) [arXiv:hep-ph/0404093].

FGS: L. Frankfurt, V. Guzey and M. Strikman, Phys. Rev. D 71 (2005) 054001 [arXiv:hep-ph/0303022].

EPS08: K. J. Eskola, H. Paukkunen and C. A. Salgado, JHEP 0807, 102 (2008) [arXiv:0802.0139 [hep-ph]].

EPS09: K. J. Eskola, H. Paukkunen and C. A. Salgado, JHEP 0904 (2009) 065 [arXiv:0902.4154 [hep-ph]].

We concentrate on EKS98 and EPS09 here

x and Q^2 Dependence of EPS09

Note that the width of the uncertainty band can be bigger than any individual ratio since the errors added in quadrature

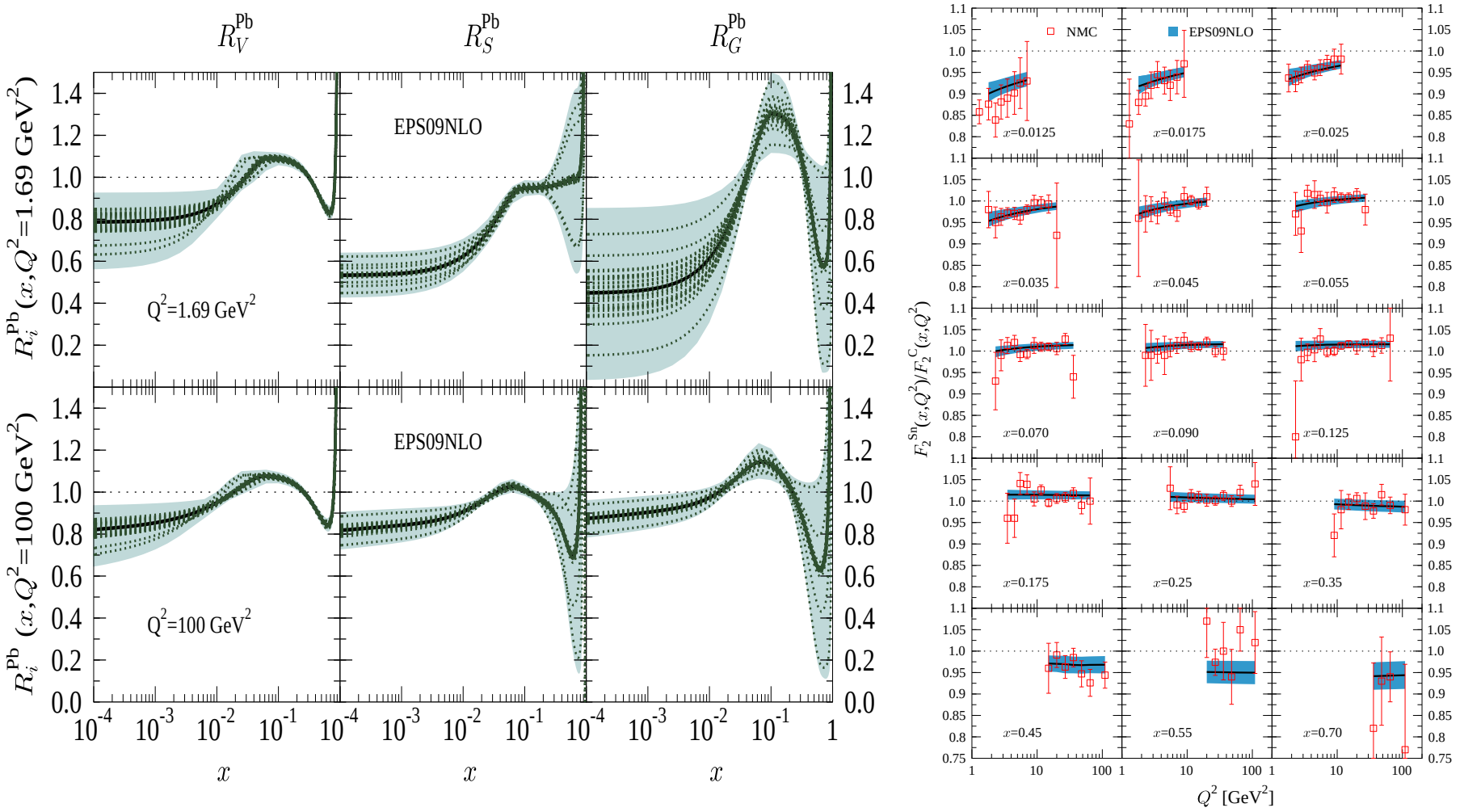

Figure 3: **Left: Gluon ratios at $Q_0^2 = 1.69$ GeV^2 (top) and 100 GeV^2 (bottom). Right: evolution of gluon distributions for several fixed values of x shows that the effect of the nonlinear terms vanishes as Q^2 increases.**

Shadowing Effects Same at LO and NLO

While the magnitude of the absolute cross sections may differ at LO and NLO, the effect of shadowing is, by design, the same at LO and NLO

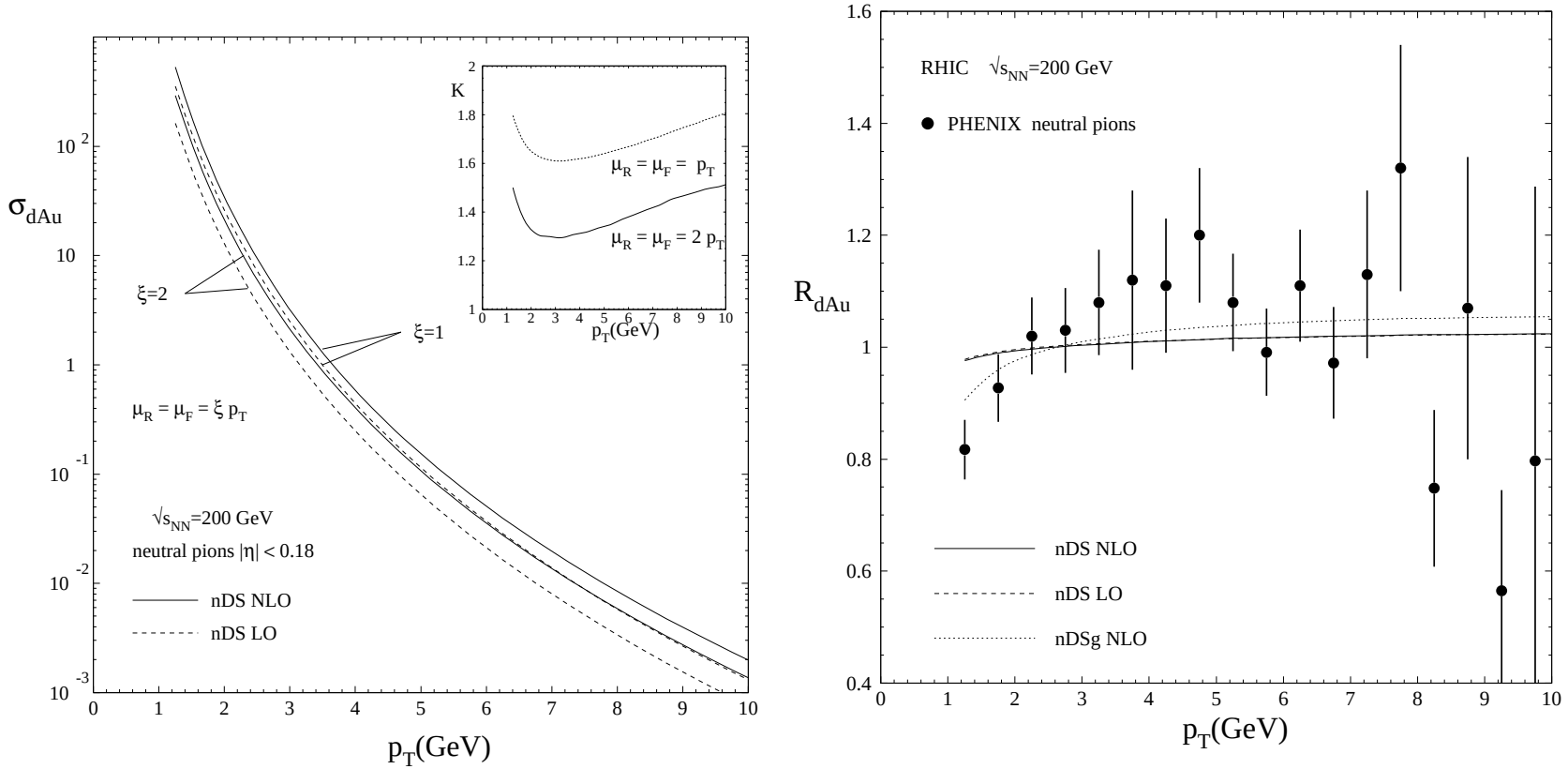

Figure 4: **Left: The π^0 cross section in d+Au collisions at $\sqrt{s_{NN}} = 200$ GeV at LO and NLO. Right: The LO and NLO calculations of $R_{\rm dAu}$.**

Comparing Shadowing Parameterizations: x Dependence

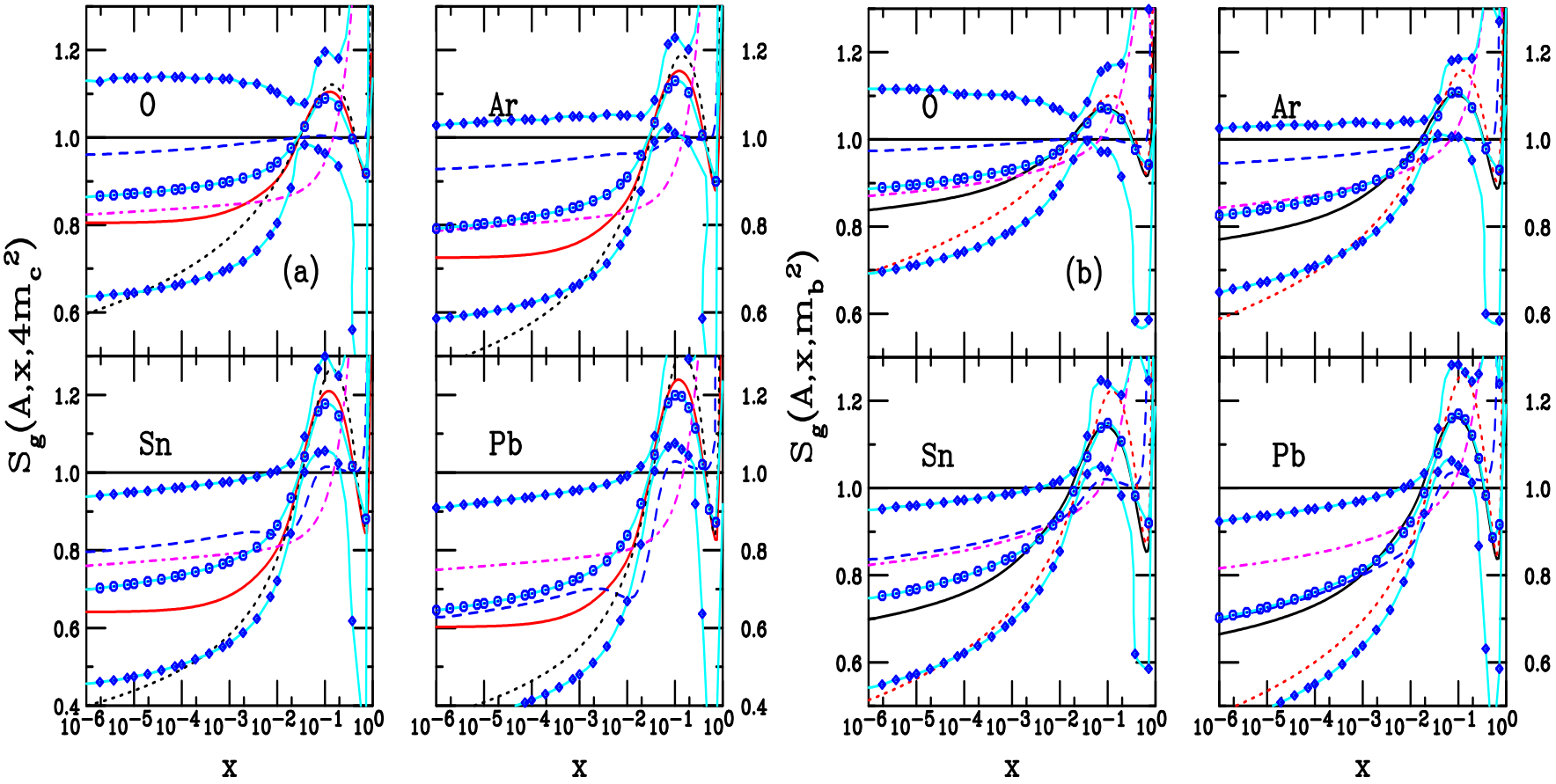

Figure 5: **Comparison of EKS98 (red), nDSg (blue), HKN (green), EPS08 (magenta), and EPS09 (cyan, with symbols) gluon shadowing parameterizations for J/ψ (left) and Υ (right) production scales with A =O, Ar, Sn and Pb.**

Predictions For J/ψ and Υ $R_{\rm dAu}$ at RHIC

Shadowing alone, no absorption; central EPS09 very similar to EKS98

Backward rapidity J/ψ data in antishadowing region, forward data in shadowing region; some absorption seems to be needed

Larger x probed for Υ production puts antishadowing peak near midrapidity, narrower y distributions than for J/ψ at same energy due to larger Υ mass (talk by Matagne)

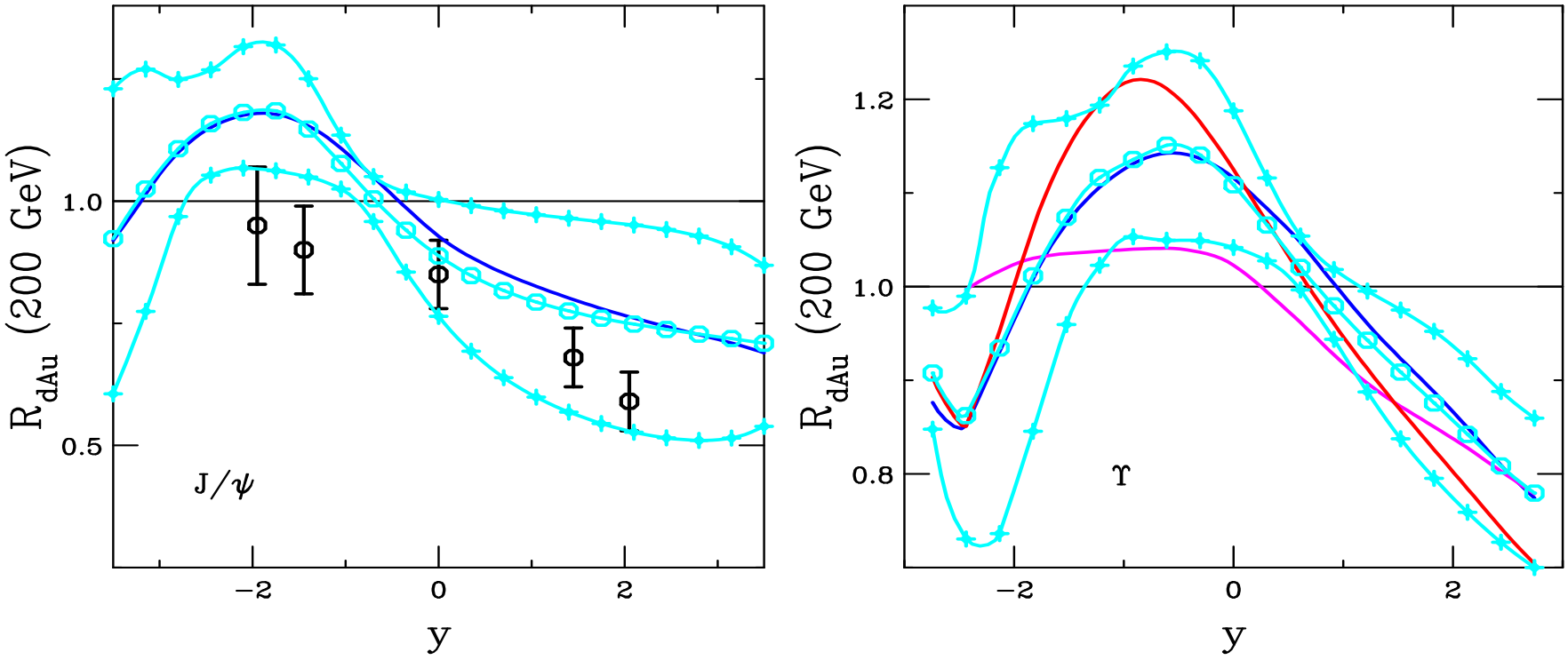

Figure 6: **The d+Au/pp minimum bias J/ψ (left) and Υ (right) ratios as a function of rapidity for the EKS98 (blue), nDSg (magenta), EPS08 (red) and EPS09 (cyan) parameterizations at 200 GeV.**

Implications of Shadowing on J/ψ Production Kinematics

pW$/pp$ ratios of J/ψ production calculated with EKS98 and no final-state absorption

Left: Dependence on $\sqrt{s_{NN}}$ at $x_F = 0$, energies of typical data indicated

Right: Dependence on x_F for three different energies; antishadowing peak narrows closer to $x_F \sim 0$; shadowing stronger at forward x_F

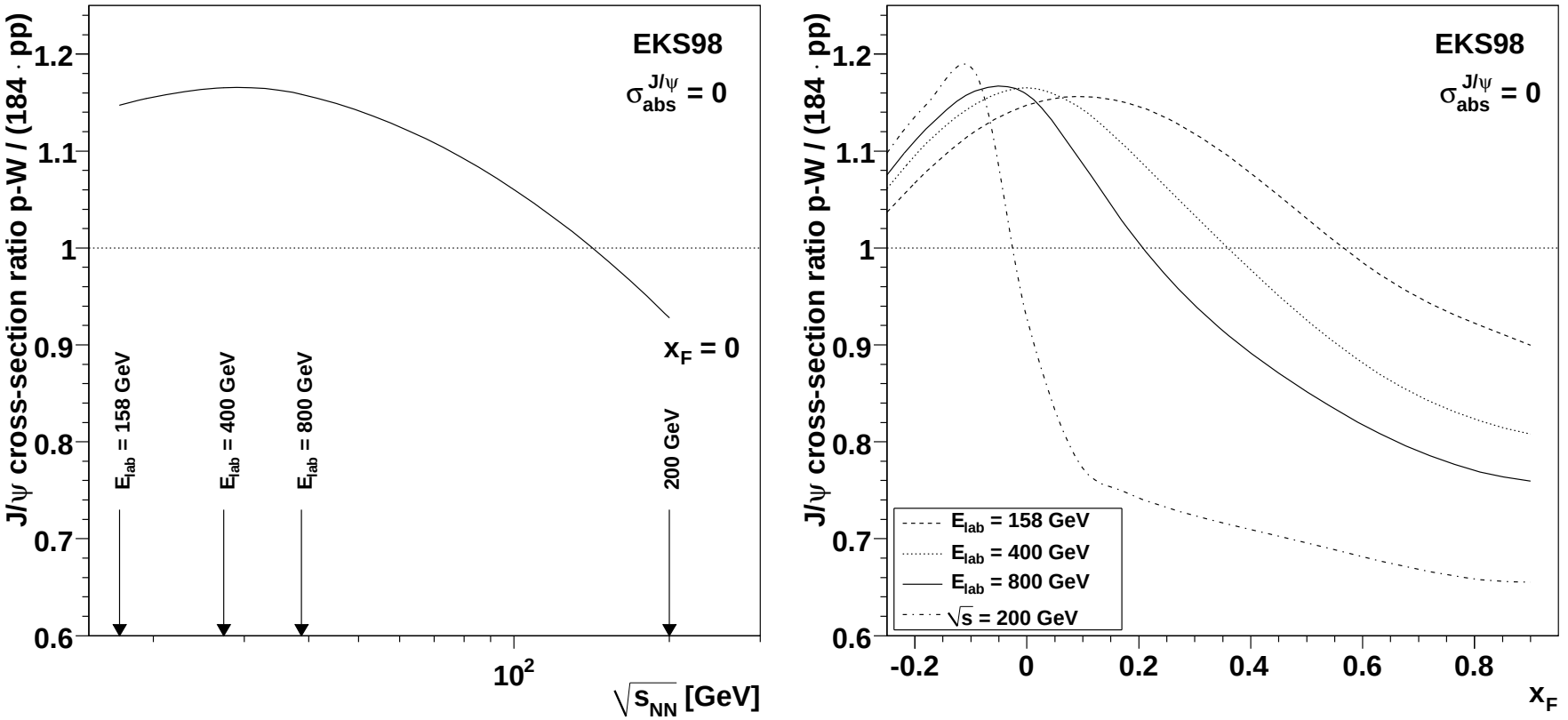

Figure 7: Changes induced by the nuclear modifications of the PDFs on the J/ψ production cross section per nucleon, in pW collisions, with EKS98, as a function of collision energy at $x_F = 0$ (left) and as a function of x_F at three proton beam energies (right). [Lourenço, RV, Wöhri]

Quarkonium Absorption by Nucleons

Woods-Saxon nuclear density profiles typically used

$$\begin{aligned}\sigma_{pA} &= \sigma_{pN}\int d^2b\int_{-\infty}^{\infty} dz\,\rho_A(b,z)S_A^{\rm abs}(b)\\ &= \sigma_{pN}\int d^2b\int_{-\infty}^{\infty} dz\,\rho_A(b,z)\exp\left\{-\int_z^{\infty} dz'\rho_A(b,z')\sigma_{\rm abs}(z'-z)\right\}\end{aligned}$$

Note that if $\rho_A=\rho_0$, $\alpha = 1-9\sigma_{\rm abs}/(16\pi r_0^2)$

Value of $\sigma_{\rm abs}$ **depends on parameterization of** σ_{pA} **– Glauber, hard sphere,** A^α **...**

Initial-state shadowing only recently taken into account at SPS energies (talk by P. Cortese)

Typically assume that each charmonium state interacts with a constant asymptotic absorption cross section assumed universal in y, $\sqrt{s}$ **and state**
Feed down to J/ψ **from** χ_c **and** ψ' **decays included by**

$$\sigma_{pA} = \sigma_{pN}\int d^2b\,[F_{\psi,\rm dir}S_{\psi,\,\rm dir}(b) + F_{\chi_{cJ}}S_{\chi_{cJ}}(b) + F_{\psi'}S_{\psi'}(b)]$$

The χ_c A **dependence remains unmeasured**

Obviously $\sigma_{\rm abs}^{\psi}\neq\sigma_{\rm abs}^{\psi'}$, **if absorption depends on size,** $\sigma_{\rm abs}^{\chi_{cJ}}$ **should be in between two – could depend on production mechanism:** χ_c **can be produced in singlet state,** J/ψ **and** ψ' **have large octet contributions in NRQCD**

Interplay of Shadowing and Absorption

Absorption alone always gives less than linear A dependence ($\alpha < 1$)

For SPS energies, $17.3 \leq \sqrt{s} \leq 29$ GeV, rapidity range covered is in EMC and antishadowing region, $\alpha > 1$ with no absorption

Adding shadowing to SPS absorption calculations requires a larger absorption cross section to maintain agreement with data

For $\sqrt{s} \geq 38$ GeV, x in shadowing regime, thus $\alpha < 1$ with shadowing alone in forward region, reducing absorption cross section needed at midrapidity

Depending on x values probed, shadowing can enhance or reduce absorption cross section needed to describe data

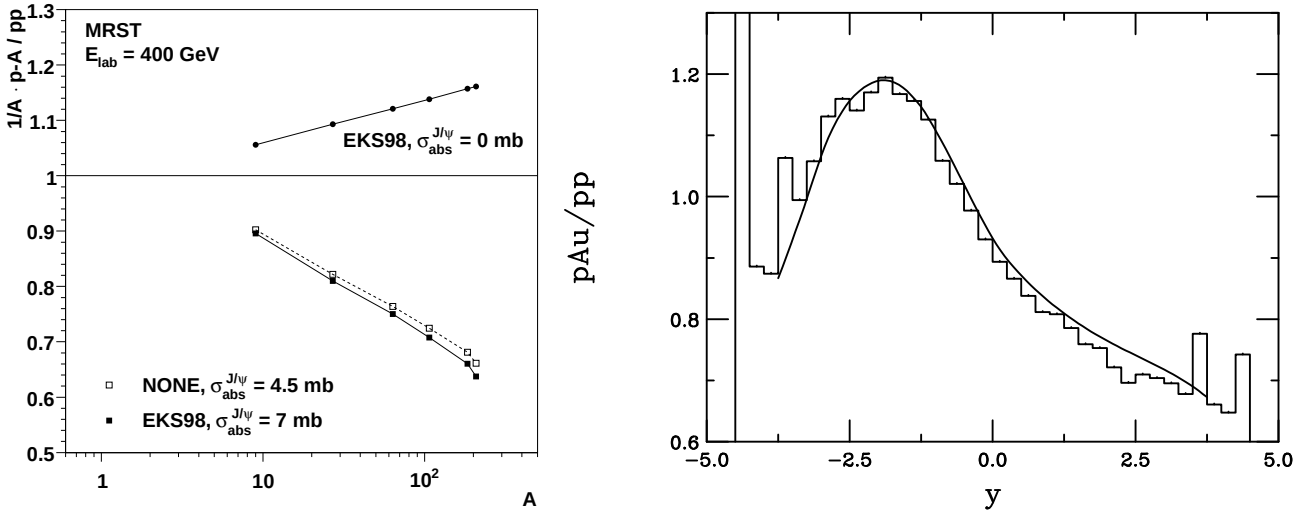

Figure 8: **(Left) Illustration of the interplay between shadowing and absorption. [C. Lourenco, H. K. Woehri and RV, JHEP 0902 (2009) 014.] (Right) Comparison of LO and NLO shadowing ratios.**

Production Mechanism Can Affect x and p_T Probed, Change Behavior of $R_{\rm dAu}$ and Extracted $\sigma_{\rm abs}$

PHENIX fits a constant "breakup" cross section common to all charmonium states assuming either EKS98 or nDSg shadowing; best fit smaller than fixed-target $\sigma_{\rm abs}$

Right-hand plot compares LO CEM calculations with CSM; shift in $R_{\rm dAu}(y)$ comes from $2 \to 2$ kinematics and higher scale in nPDFs

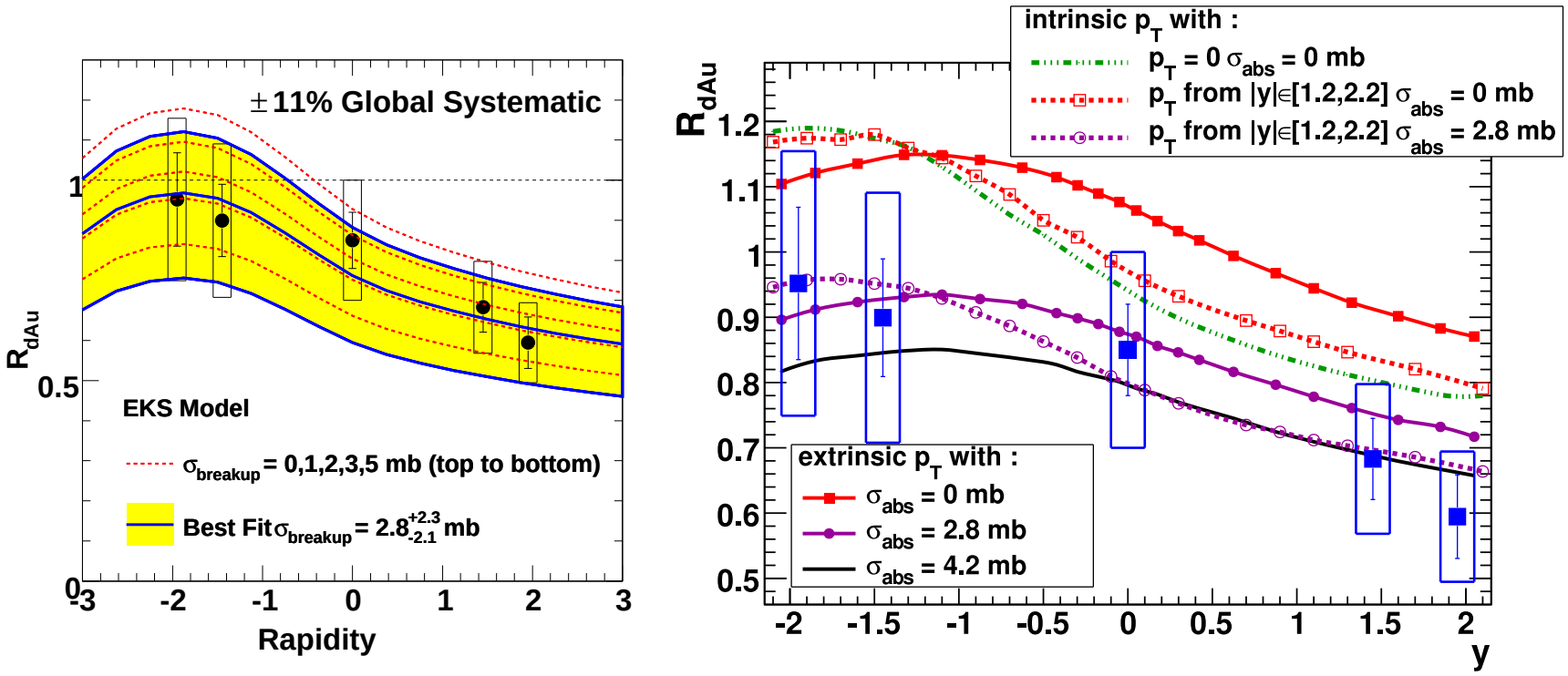

Figure 9: (Left) The d+Au/pp minimum bias ratio as a function of rapidity for EKS98. A range of breakup cross sections ($\sigma_{\rm breakup}$ = 0, 1, 2, 3 and 5 mb) are shown, as well as a best fit band consistent with the data to one standard deviation. [PHENIX, Phys. Rev. C **77** (2008) 024912; erratum 0903.4845v1.] (Right) $R_{\rm dAu}$ calculated in LO CEM (dashed) and s-cut CSM (solid) for several values of $\sigma_{\rm abs}$. [E. G. Ferreiro *et al.*, arXiv:0809.4684.]

PHENIX 200 GeV $R_{\mathrm{dAu}}(N_{\mathrm{coll}})$ and $R_{CP}(y)$

Largest model difference for fixed σ_{abs} is in antishadowing region ($y = -1.7$)

PHENIX fits using different $\sigma_{\mathrm{breakup}}$ in each rapidity interval

New R_{CP} data show improvement in statistics from latest run

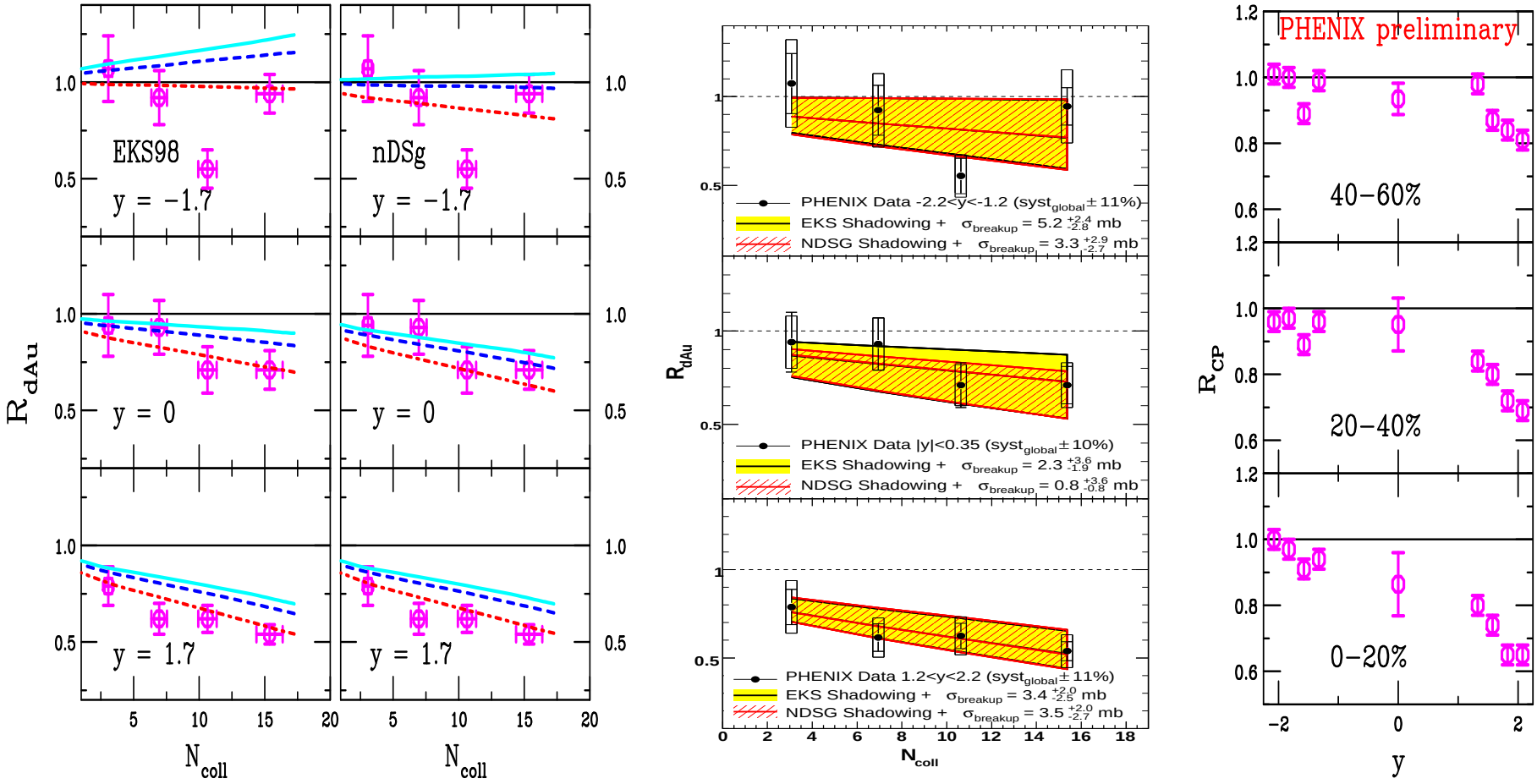

Figure 10: (Left) The dAu/pp ratio as a function of the number of collisions calculated with EKS98 (left) and nDSg (right) with the MRST2001 PDFs. The curves are for $\sigma_{\mathrm{abs}}^{J/\psi} = 0.5$ (solid blue) and 1.75 mb (dashed red). PHENIX data are shown for d+Au collisions at 200 GeV for $y = -1.7$ (top), 0 (middle) and 1.7 (bottom). (Center) PHENIX plot showing the EKS98 and nDSg parameterizations with the breakup cross sections fit in each rapidity interval. [PHENIX, Phys. Rev. C **77** (2008) 024912; erratum 0903.4845v1.] (Right) PHENIX R_{CP} in d+Au collisions. [PHENIX, Quark Matter 2009.]

Is $\sigma_{\rm abs}^{J/\psi}$ Energy Dependent?

Asymmetric Gaussians used to fit $x_F < 0.25$ region of E866 and HERA-B data

Shapes at other energies determined by fits, magnitude adjusted to data: $\sigma_{\rm abs}^{J/\psi}$ seems to decrease with energy

Even with no shadowing effects included (left-hand side), there seems to be a systematic decrease of the absorption cross section with energy

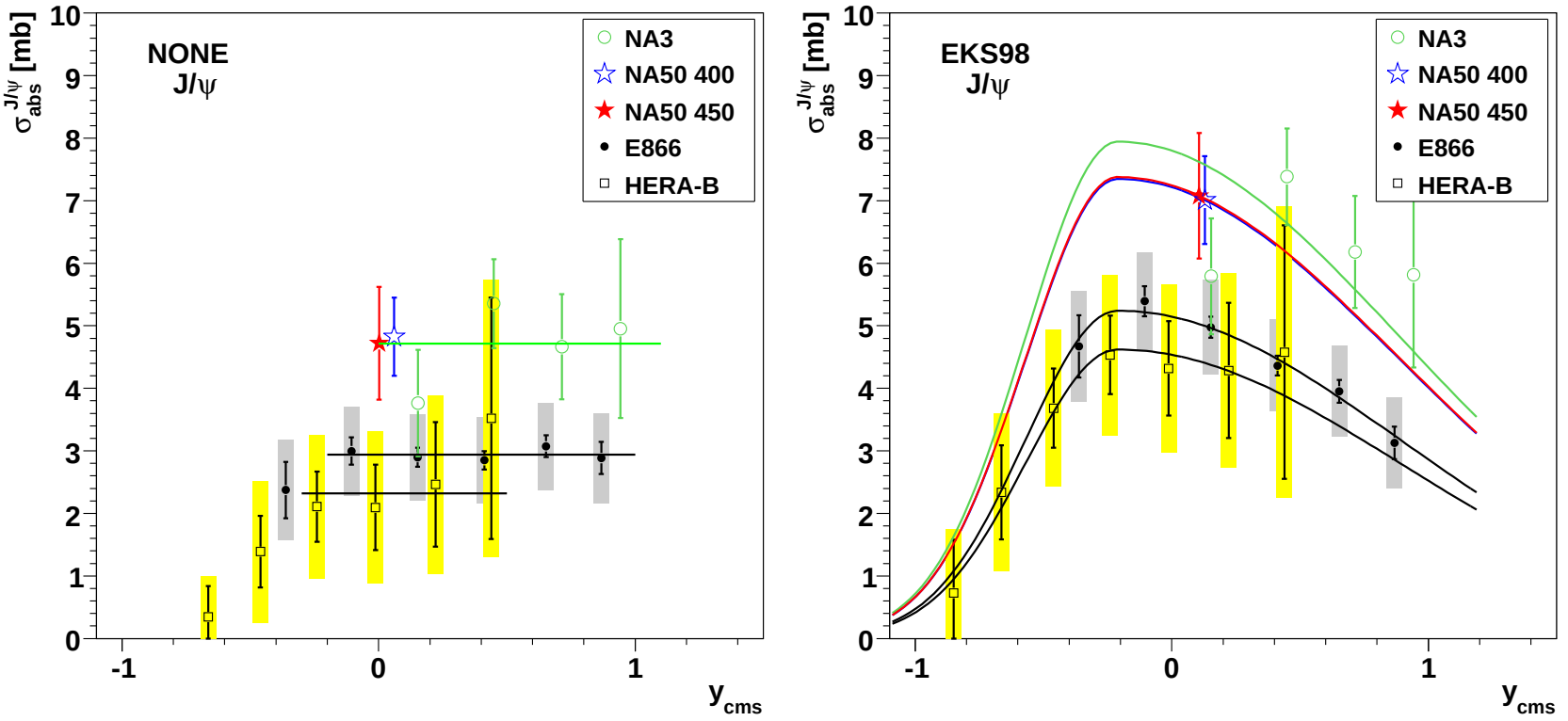

Figure 11: Dependence of $\sigma_{\rm abs}^{J/\psi}$ on $y_{\rm cms}$ for all available data sets. The shape of the curves is fixed by the E866 and HERA-B data. [Lourenço, RV, Wöhri] Left: Assuming no shadowing effects on the PDFs. Right: Including EPS98 shadowing.

Quantifying Energy Dependence of $\sigma_{\rm abs}^{J/\psi}$

$\sigma_{\rm abs}^{J/\psi}(y_{\rm cms}=0)$ decreases with $\sqrt{s_{NN}}$

$\sigma_{\rm abs}^{J/\psi}(y_{\rm cms}=0)$ extrapolated to 158 GeV is significantly larger than measured at 450 GeV, underestimating "normal nuclear absorption" in SPS heavy-ion data

Trend confirmed by NA60 pA measurements at 158 GeV (talk by P. Cortese)

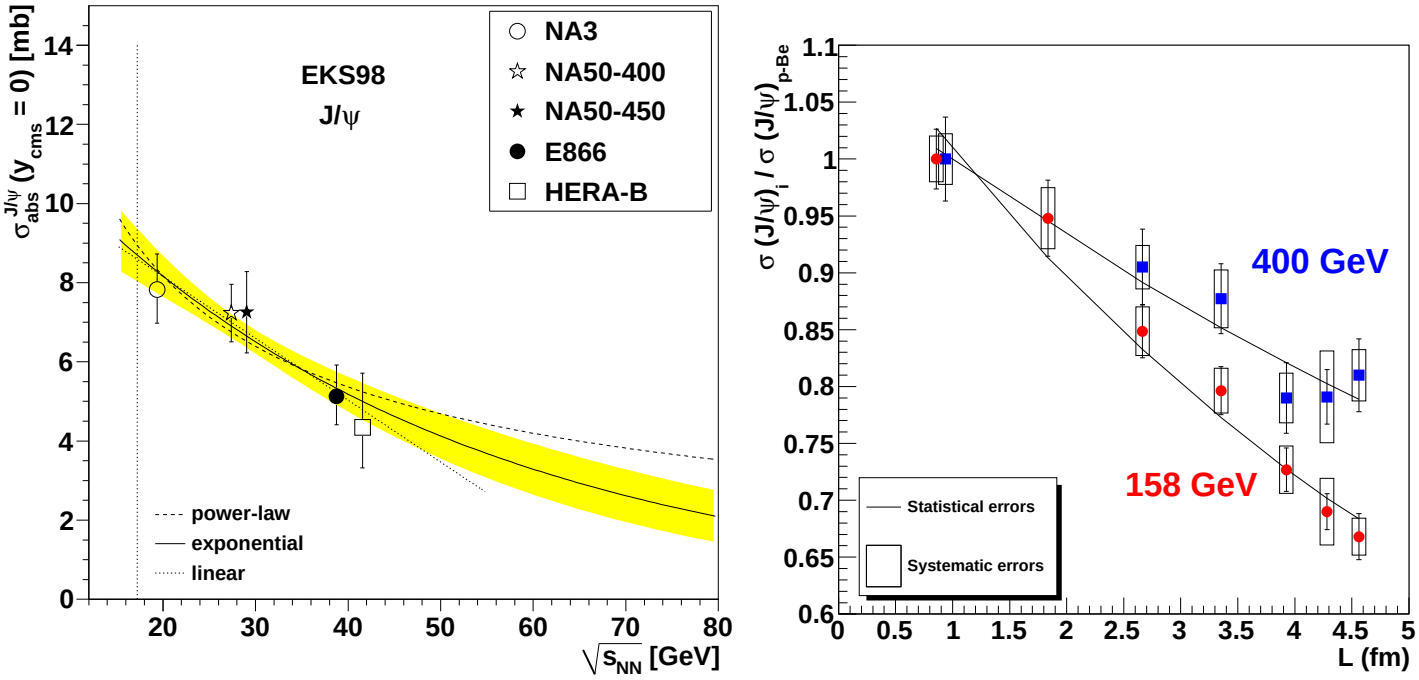

Figure 12: Left: The extracted energy dependence of $\sigma_{\rm abs}^{J/\psi}$ at midrapidity for power law (dashed), exponential (solid) and linear (dotted) approximations to $\sigma_{\rm abs}^{J/\psi}(y=0,\sqrt{s_{NN}})$ using the EKS98 shadowing parameterization with the CTEQ61L parton densities. The band around the exponential curve indicates the uncertainty in the extracted cross sections at $x_F \sim 0$ from NA3, NA50 at 400 and 450 GeV, E866 and HERA-B. The vertical dotted line indicates the energy of the Pb+Pb and In+In collisions at the CERN SPS. [Lourenço, RV, Wöhri] Right: The J/ψ cross section ratios for pA collisions at 158 GeV (circles) and 400 GeV (squares), as a function of L, the mean thickness of nuclear matter traversed by the J/ψ. [Arnaldi, Cortese, Scomparin]

Rapidity Dependence of $\sigma_{\rm abs}^{J/\psi}$ Shows Holes in Our Understanding

Away from midrapidity, data more complex: strongly increased absorption

NA60 data rise at lower y than higher energy results from E866 and PHENIX

Such strong effects can't come from any of the shadowing parameterizations

CSM results give smaller $\sigma_{\rm abs}$ but exhibit same trend

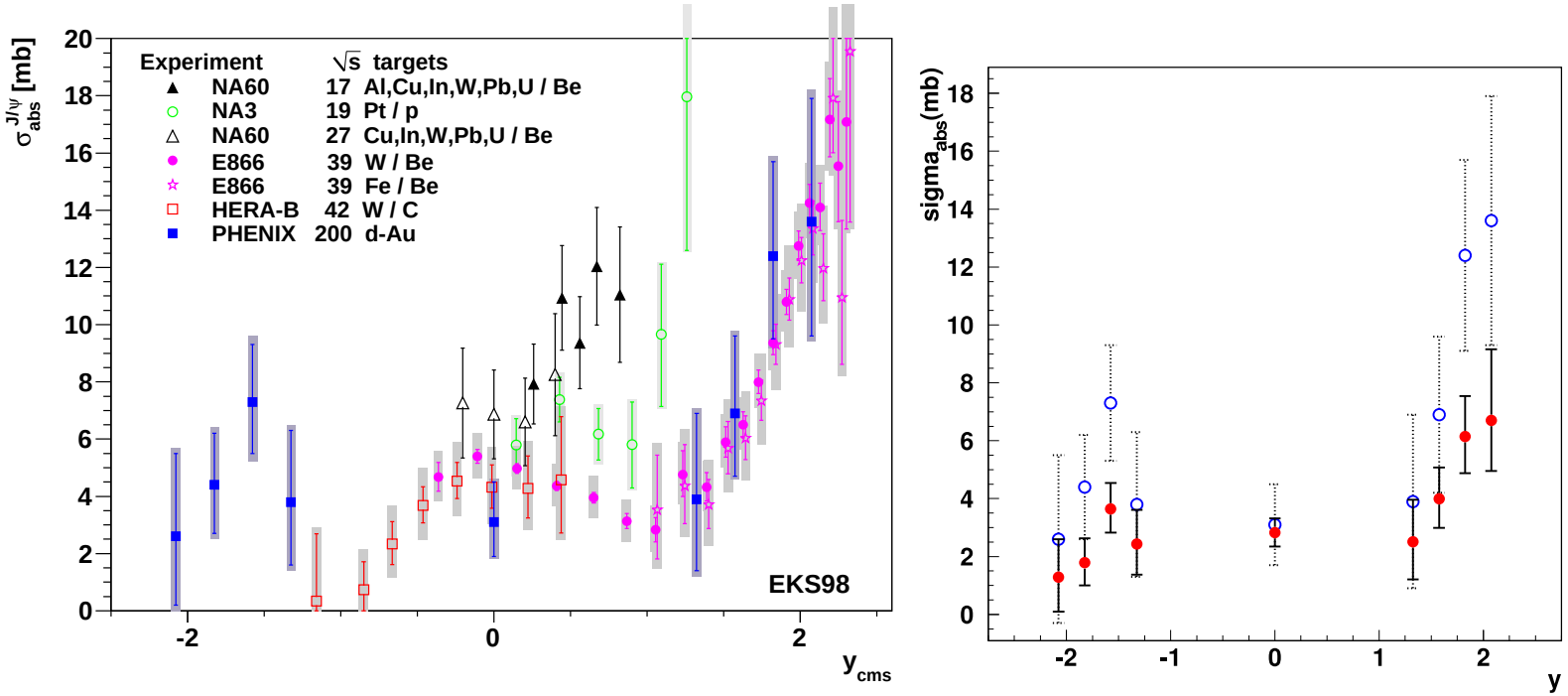

Figure 13: Left: The center-of-mass rapidity dependence of $\sigma_{\rm abs}^{J/\psi}$ for incident fixed-target energies from 158, 200, 400, 450, 800, 920 GeV and preliminary PHENIX results from RHIC obtained using the EKS98 shadowing parameterization. (Plot made by Hermine Wöhri with PHENIX data from Tony Frawley.) Right: Comparison of PHENIX results using CEM with CSM (Ferreiro *et al.*).

Experimental Heavy/Light Ratios Confirm Effect

Rather wide range of EPS09 uncertainty reduced in ratios; clearly initial-state shadowing must be supplemented by other mechanisms

Initial state energy loss? Needs to be correlated with possible quark energy loss level in NLO DY production, work in progress with C. Lourenco, H. Wöhri and P. Faccioli

Away from midrapidity, the J/ψ and open charm measurements behave similarly, as might be expected from an initial-state effect

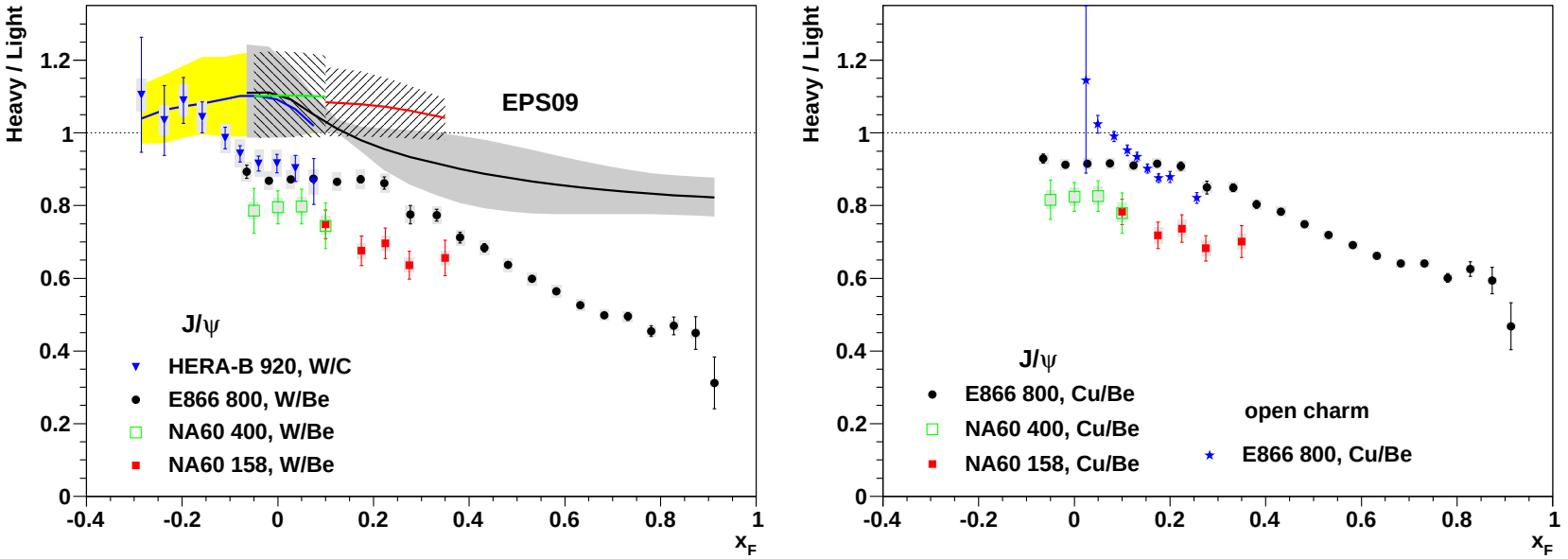

Figure 14: The heavy to light ratios for W/Be (left) as well as for Fe/Be and Cu/Be (right) in fixed target interactions. The right-hand figure also includes preliminary E866 open charm data.

Extracting Cold Matter Effects on Quarkonium May Be More Difficult at LHC

Initial J/ψ and Υ yields will be large but nuclear effects harder to interpret

- **pA interactions likely to be run in equal-speed frame rather than at same energy as AA system**
- **Center-of-mass rapidity shifted from $y = 0$ in equal-speed frame**
- **pp reference data most likely to be available first at 14 TeV**
- **Need to take higher energy reference and pA rapidity shift into account**
- **Smaller shift in dA collisions but need second ion source, not likely soon**

A	E_A (TeV)	y_A	$\sqrt{s_{_{NN}}}$ (TeV)	$y^{pA}_{\rm diff}$	$\Delta y^{pA}_{\rm cm}$	$\sqrt{s_{_{NN}}}$ (TeV)	$y^{{\rm d}A}_{\rm diff}$	$\Delta y^{{\rm d}A}_{\rm cm}$	$\sqrt{s_{_{NN}}}$ (TeV)
			pA			dA			AA
O	**3.5**	**8.92**	**9.9**	**0.690**	**0.345**	**7**	**0**	**0**	**7**
Ar	**3.15**	**8.81**	**9.39**	**0.798**	**0.399**	**6.64**	**0.052**	**0.026**	**6.3**
Kr	**3.07**	**8.79**	**9.27**	**0.824**	**0.412**	**6.48**	**0.077**	**0.038**	**6.14**
Sn	**2.92**	**8.74**	**9.0**	**0.874**	**0.437**	**6.41**	**0.087**	**0.043**	**5.84**
Pb	**2.75**	**8.67**	**8.8**	**0.934**	**0.467**	**6.22**	**0.119**	**0.059**	**5.5**

Table 1: For each ion species at the LHC, the maximum beam energy per nucleon and the corresponding beam rapidity. Using the maximum proton or deuteron beam energy: $E_p = 7$ TeV and $y_p = 9.61$; $E_{\rm d} = 3.5$ TeV and $y_{\rm d} = 8.92$ respectively, we present the maximum center-of-mass energy, rapidity difference, $y^{iA}_{\rm diff} = y_i - y_A$ ($i = p$, d) and center-of-mass rapidity shift, $\Delta y^{iA}_{\rm cm} = y^{iA}_{\rm diff}/2$, for pA, dA and AA collisions. Note that there is no rapidity shift in the symmetric AA case.

Absorption Cross Section Negligible at LHC Energies?

Extrapolating our energy dependence, expect $\sigma_{\rm abs}^{J/\psi} << 1$ mb in pA collisions at LHC

Shadowing effects somewhat washed out with higher energy reference; rapidity shift flattens all ratios somewhat but ratios still different than no shadowing

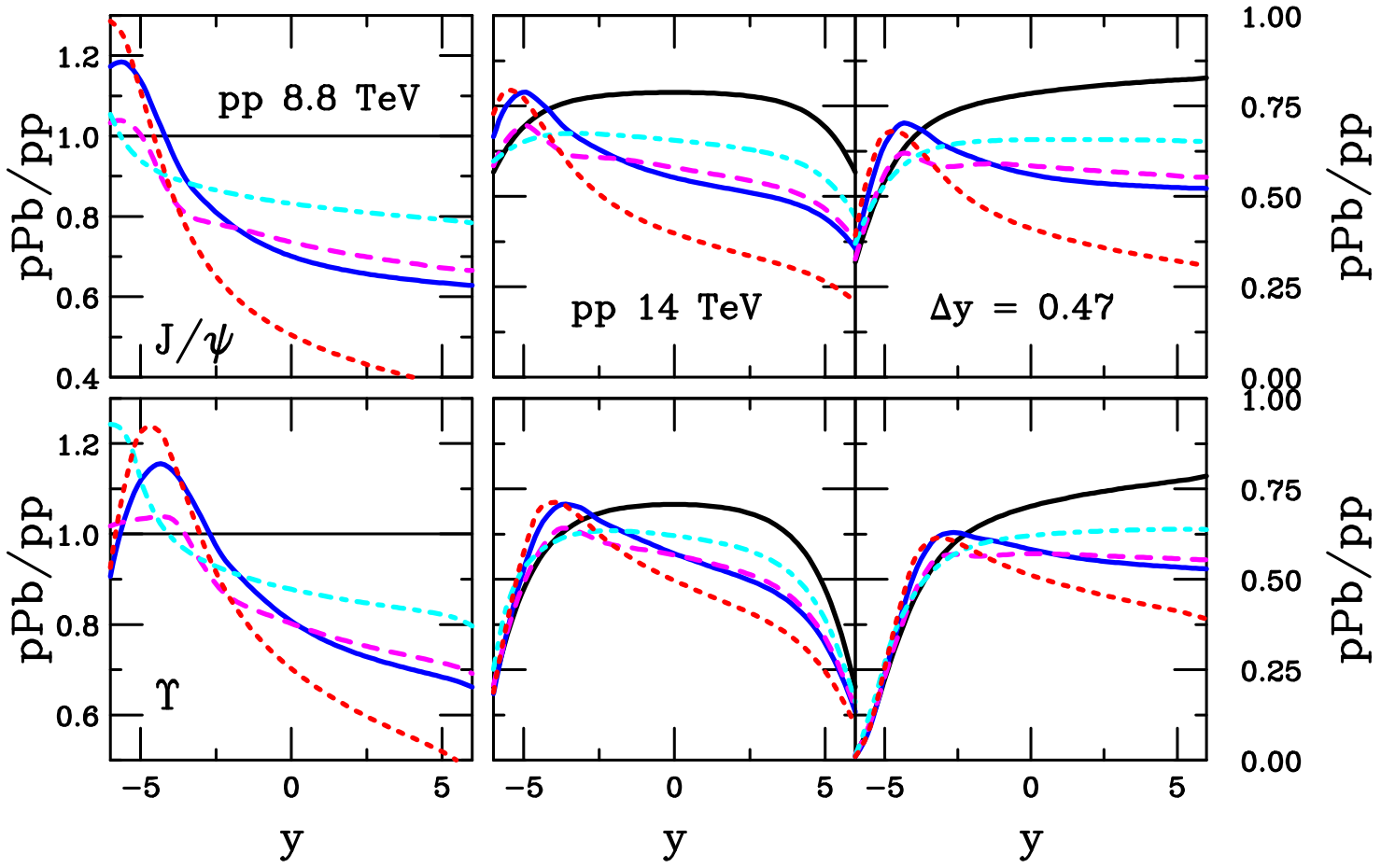

Figure 15: The pPb/pp ratios for J/ψ (top) and Υ (bottom) production at 8.8 TeV for: pA and pp collisions at the same center-of-mass energy and $\Delta y = 0$ (left); the pp reference at 14 TeV with $\Delta y = 0$ (center); and the higher energy pp reference and pA rapidity shift in the equal-speed frame taken into account (right). The curves show EKS98 (blue solid), nDSg (magenta dashed), HKN (cyan dot-dashed) and EPS08 (red dotted) shadowing parameterizations with no nuclear absorption. The black curves in the center and right panels show the ratios with no shadowing.

Advantage in Using dA to Study Cold Matter Effects

d+Pb closer to Pb+Pb energy, lower ratio relative to pp but d beam makes almost negligible rapidity shift

Ratios turn over at high y because pp rapidity distribution is broader

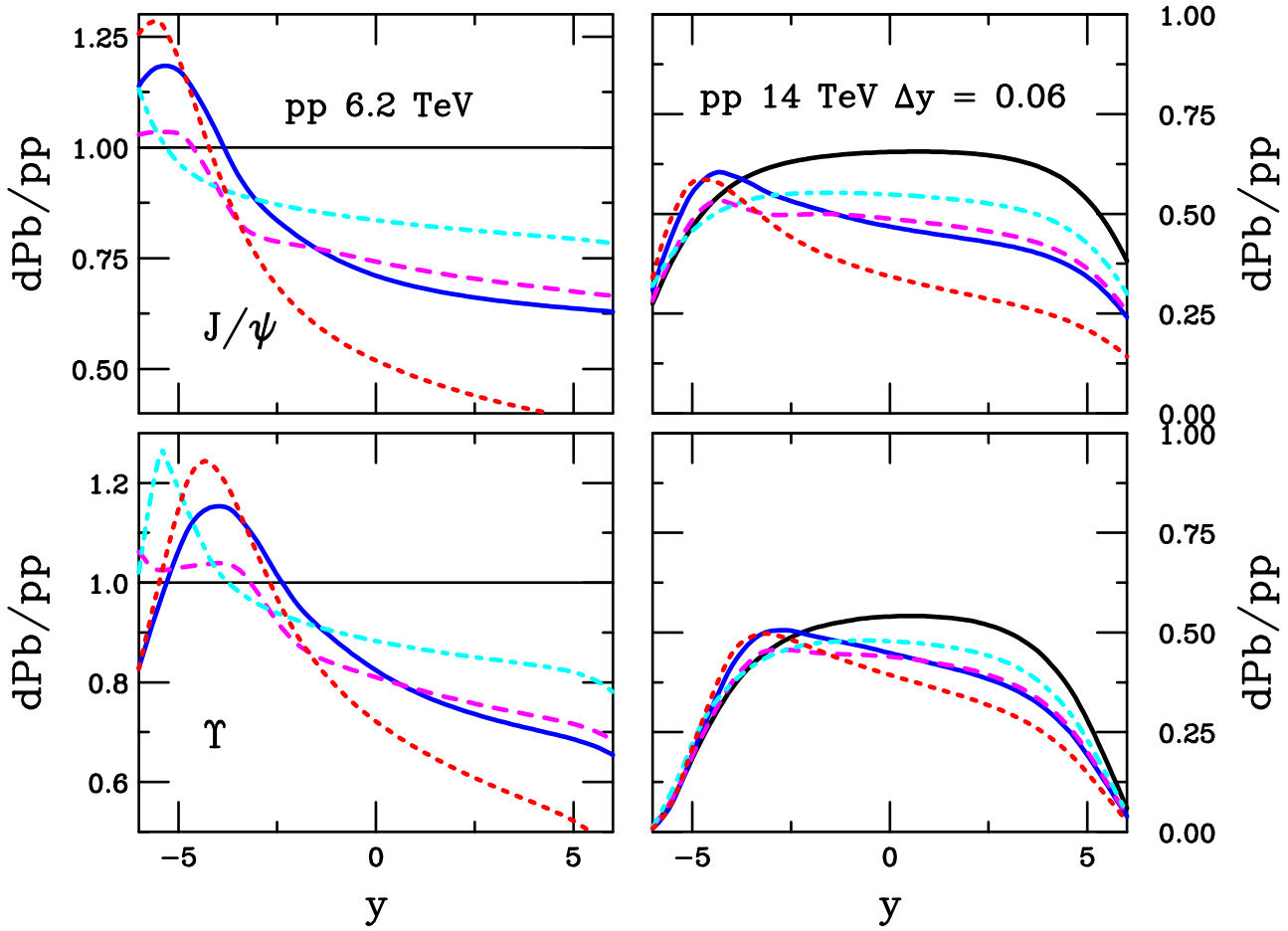

Figure 16: The d+Pb/pp ratios for J/ψ (top) and Υ (bottom) production at 6.2 TeV for: d+Pb and pp collisions at the same center-of-mass energy and $\Delta y = 0$ (left); the pp reference at 14 TeV with the small d+Pb rapidity shift taken into account (right). The curves show EKS98 (blue solid), nDSg (magenta dashed), HKN (cyan dot-dashed) and EPS08 (red dotted) shadowing parameterizations with no nuclear absorption. The black curves in the right panels show the ratios with no shadowing.

Predictions for $R_{\rm dPb}(b)$ and $R_{CP}(y)$ at the LHC

R_{CP} can be used to trace out shadowing function when pp data at same energy not available

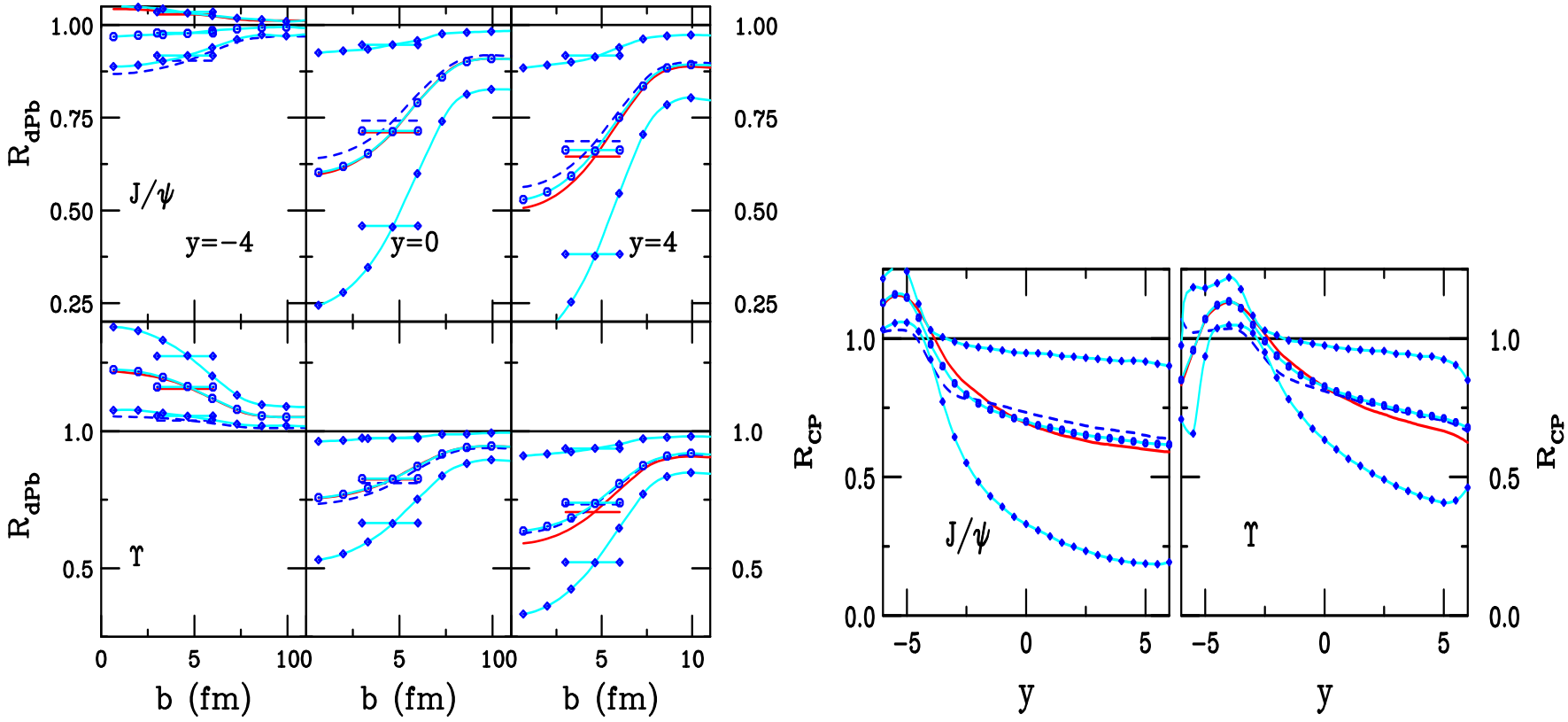

Figure 17: (Left) The suppression factor $R_{\rm dPb}$ at $y = -4$ (left), 0 (center) and 4 (right) as a function of b. The result is shown for J/ψ (top) and Υ (bottom) in d+Pb relative to $p + p$ collisions at the same energy, $\sqrt{s_{NN}} = 6.2$ TeV, and employ the EKS98 (solid), nDSg (dashed) and EPS09 (solid curves with symbols) shadowing parameterizations. The horizontal lines show the impact-parameter integrated results. (Right) The central-to-peripheral ratios, R_{CP}, as a function of rapidity for $b_P \approx R_A$ relative to $b = 0$ for d+Pb collisions at $\sqrt{s_{NN}} = 6.2$ TeV. The calculations are with CTEQ6 and employ the EKS98 (solid), nDSg (dashed) and EPS09 (solid curves with symbols) shadowing parameterizations.

Summary

- Data clearly show that J/ψ and ψ' have different A dependence, translates into different effective absorption for J/ψ and ψ'
- SPS shadowing and absorption calculations show larger absorption cross sections needed to counter antishadowing effects but $\sigma_{\rm abs}^{J/\psi}$ smaller overall if $\sigma_{\rm abs}^{\psi'} > \sigma_{\rm abs}^{J/\psi}$
- Measurement of χ_c A dependence would provide additional test of production and absorption mechanisms
- Data seem to suggest absorption cross section decreases with $\sqrt{s_{NN}}$ and increases at forward x_F with a strength depending on the production mechanism, work in progress to understand why
- Need better statistics to distinguish between shadowing parameterizations and determine strength of absorption at RHIC, expected from soon to be released PHENIX d+Au data (next talk)